

# Characterization of Deep Surface-Opening Cracks in Concrete: Feasibility of Impact-Generated Rayleigh-Waves

by Hwa Kian Chai, Shohei Momoki, Dimitrios G. Aggelis, and Tomoki Shiotani

*The feasibility of impact-generated Rayleigh waves (R-waves) for measuring deep surface-opening cracks in concrete structures was studied. The aim is to contribute to a methodology for simple and effective in-place crack depth estimation. Specimens induced with vertical slits of different depths were prepared for measurement. A two-sensor array was implemented and elastic waves of different central frequencies were generated by mechanical impacts with steel-ball hammers of different ball diameters. R-wave amplitudes were extracted from the waveforms. Attenuation of R-waves due to diffraction and scattering by the slits and the trend of amplitude decaying with slit depth were examined. A reasonable correlation between the amplitude factor and slit depth-to-wavelength ratio was established, which indicated the loss of sensitivity in the change of amplitude factor with regard to dominant wavelengths smaller than the slit depth. By comparing the results of P-wave time-of-flight (TOF) method, the results by measuring again using the proposed method confirmed the feasibility of R-wave attenuation as an alternative parameter for characterizing surface-opening cracks. In addition, it was also demonstrated potential problems associated with the reliability of P-wave TOF method in estimating a crack with limited length.*

**Keywords:** amplitude factor; attenuation; nondestructive testing; Rayleigh waves; surface-opening cracks.

## INTRODUCTION

Concrete structures are susceptible to various forms of attacks including applied load, drying shrinkage, temperature variation, steel corrosion and other forms of degradation. Surface cracking is one of the most common forms of defect found in concrete structures as a consequence of the attacks. Depending on the extent and their locations, surface-opening cracks pose different levels of threats in degrading the overall strength and durability performance of the structure. To make things worse, these cracks, if they penetrate through the thickness of the concrete cover, could result in exposure of steel reinforcement and facilitate the ingress of chloride to accelerate the corrosion process.<sup>1</sup> Effective detection and evaluation of surface-opening cracks are vital so that appropriate repair or strengthening can be conducted to restore structural integrity. Several nondestructive tests (NDT) have been developed to detect surface-opening cracks in concrete structures. The ultrasonic time-of-flight (TOF) method is the most straightforward to adopt, in which the time and distance of compression wave (P-wave) propagation are used to compute the velocity, so that anomalies that cause delay in the wave propagation can be identified. Van Hauwaert et. al.<sup>2</sup> conducted a study to follow cracks developed under bending of reinforced concrete (RC) members by establishing a direct relation between the variation of ultrasonic parameters during crack growth and the crack length. There are also reports on the development of ultrasonic spectroscopy for evaluating cracks and an ultrasonic imaging method that

scans the concrete surface for cracking.<sup>3-5</sup> A similar method to the ultrasonic TOF method was developed by using elastic waves induced by mechanical impacts, in which the travel time of P-waves of known velocity diffracted from crack tip were measured to calculate the depth of crack.<sup>6,7</sup> In most real cases, however, the crack surfaces were filled with water and dust or in contact with the opposite surface, as well as in connection with steel reinforcements. The filling, contact, or connection can carry the P-waves across the cracks. Therefore, when identifying the depth of cracks, especially those with great depths, underestimation can commonly occur due to the shorter-than-expected wave path through the bridging points.<sup>8</sup>

Recently, studies on the use of Rayleigh wave (R-wave) scattering and attenuation characteristics in estimating depths of surface-opening cracks in concrete have been reported.<sup>9-16</sup> R-waves propagate the surface of an object with a penetration depth of approximately one wavelength. Furthermore, R-waves carry a higher amount of energy than bulk waves, that is, approximately 67% of the total energy of elastic waves, and have a low attenuation rate in geometric spreading due to their cylindrical wavefront, which enable them to propagate over longer distances than the bulk waves.<sup>9</sup> Also, unlike P-waves, the cylindrical particle movements of R-waves, which are perpendicular to the propagation direction, depend heavily on the shear properties of the medium.<sup>14</sup> Therefore, the existence of steel bar, water, or dust, as well as contact between aggregates inside a crack, are not expected to affect the wave propagation because of insignificant shear properties of the substance and contact surface.

Most of the studies for R-waves, experimentally or analytically, have been linked with evaluating concrete cracks that are relatively shallow in depth. In these studies, measurements by ultrasonic excitations of high frequencies were conducted. Although signal processing and identification for crack evaluation can be precisely performed with high consistency due to the good sensitivity of high frequency waves toward attenuation, penetration of wave energy into concrete has been very limited due to the short wavelength of the ultrasonic waves. It is also known that the relation between amplitude decay and crack depth can be established by taking the ratio between crack depth and wavelength; therefore, the relation is not confined to a certain range of crack depth, that is, varying the wavelength enables crack-depth evaluation of any scale.<sup>9-13,17</sup> There is still a lack of experimental data, however, to confirm the effectiveness of

*ACI Materials Journal*, V. 107, No. 3, May-June 2010.

MS No. M-2009-227 received June 29, 2009, and reviewed under Institute publication policies. Copyright © 2010, American Concrete Institute. All rights reserved, including the making of copies unless permission is obtained from the copyright proprietors. Pertinent discussion including authors' closure, if any, will be published in the March-April 2011 *ACI Materials Journal* if the discussion is received by December 1, 2010.

**Hwa Kian Chai** is a Research Engineer at the Research Institute of Technology, Tobishima Corporation, Chiba, Japan. He received his BEng in civil engineering from the University Science Malaysia, Pulau Pinang, Malaysia; his MEngSc in concrete materials from the University of Malaya, Kuala Lumpur, Malaysia; and his PhD in civil engineering from Osaka University, Osaka, Japan. His research interests include durability of concrete, fiber-reinforced polymer strengthening, and nondestructive testing of concrete structures.

**Shohei Momoki** is a Research Engineer at the Research Institute of Technology, Tobishima Corporation, Chiba, Japan. He received his bachelor's and master's degrees in agricultural engineering from Kyoto University, Kyoto, Japan. His research interests include health monitoring, damage imaging, and evaluation of concrete structures using stress wave methods.

**Dimitrios G. Aggelis** is an Assistant Professor in the Material Science and Technology Department of the University of Ioannina, Ioannina, Greece. He received his diploma in mechanical engineering and his PhD in nondestructive testing of concrete from the University of Patras, Patras, Greece. His research interests include concrete damage material characterization using stress wave propagation techniques.

**Tomoki Shiotani** is an Associate Professor in the Graduate School of Engineering at Kyoto University. He received his BS and MSc from the Civil Engineering Department of the University of Tokushima, Tokushima, Japan, and his PhD from the Department of Natural Science at Kumamoto University, Kumamoto, Japan. His research interests include damage characterization of civil infrastructures using stress waves, for example, acoustic emission and elastic wave tomography.

R-waves in assessing deep surface-opening cracks usually found in large-scale concrete infrastructures, leaving the fact that a practical methodology to evaluate crack depth with R-waves is yet to be established.

This study investigates the feasibility of using R-waves to identify deep surface-opening cracks in concrete. Within the

context of this study, deep surface-opening cracks are referred to as cracks with depths equal to or greater than the concrete cover, assuming the minimum concrete cover for normal steel-RC members exposed to moderate service conditions to be in the range of 200 to 500 mm (7.87 to 19.69 in.) by taking into consideration the diameters of the most commonly used steel bars.<sup>18,19</sup> Furthermore, for nonreinforced concrete, such as that found in tunnels or dams, a crack can be considered deep relative to the dimension of the structure, in a way that it raises concerns for impairment of structural stiffness. Experiments were carried out on concrete block specimens containing vertical slits of varying depths. To facilitate comparison, depth estimations using the P-wave TOF method were also performed. In the data analysis of R-waves, the trends of R-wave amplitudes decaying with respect to slit depth were examined and correlations between the amplitude factor and the slit depth-to-wavelength ratio were established. Verification tests were then carried out and the correlations, in the form of exponential curves, were used to estimate the depth of slits. With reference to the experimental results, the feasibility of using R-wave attenuation characteristics as an alternative parameter for identifying surface-opening cracks is discussed.

## RESEARCH SIGNIFICANCE

The significance of this study lies in its experimental program to use R-waves for estimating the depth of surface-opening cracks. Cracks with depths equivalent to or greater than the concrete cover for structures under moderate service conditions, or detrimental enough to instigate loss of structural function, were considered. Excitations by mechanical impacts from steel-ball hammers produced R-waves of relatively high energy and long wavelength to enable deeper penetration and enhance sound-to-noise ratio for easy signal detection. By adopting a simple two-sensor approach, fast execution can be achieved in-place. The finding of this study offers further insight to effectively using R-waves for reliable nondestructive evaluation of concrete structures.

## EXPERIMENTAL INVESTIGATION

### Materials and specimens

Two concrete cubes 1 m (3.28 ft) in size, Specimens A and B, were prepared for testing. Artificial cracks, in the form of vertical slits of 300 mm (11.81 in.) long, 0.4 mm (0.016 in.) wide, and of varying depths  $d$  were introduced into the specimens. Figure 1 shows the details of both specimens to indicate the locations of slits. The slits were formed by removing thin metal plates of different dimensions, which were inserted into the concrete formwork prior to casting, at the third day after the casting. Three sides of Specimen A had slits with depths of 50, 80, 100, 130, and 150 mm (1.97, 3.15, 3.94, 5.12, and 5.91 in.), whereas the fourth side was free of slits to serve as the sound portion. In Specimen B, slits with greater depths, that is, 200, 250, 300, 350, 400, and 500 mm (7.87, 9.84, 11.81, 13.78, 15.75, and 19.69 in.) were created.

Table 1 gives the concrete mixture proportions of the specimens. The concrete mixture was prepared using ordinary portland cement, a maximum aggregate size of 20 mm (0.787 in.), and 4.5% entrained air. After casting, the specimens were cured under air-dried conditions. At 28 days, the concrete achieved an average compressive strength of 29.1 MPa (4220.60 psi) and a Young's modulus of 26.4 GPa (3,828,996.28 psi) based on testing procedures as prescribed

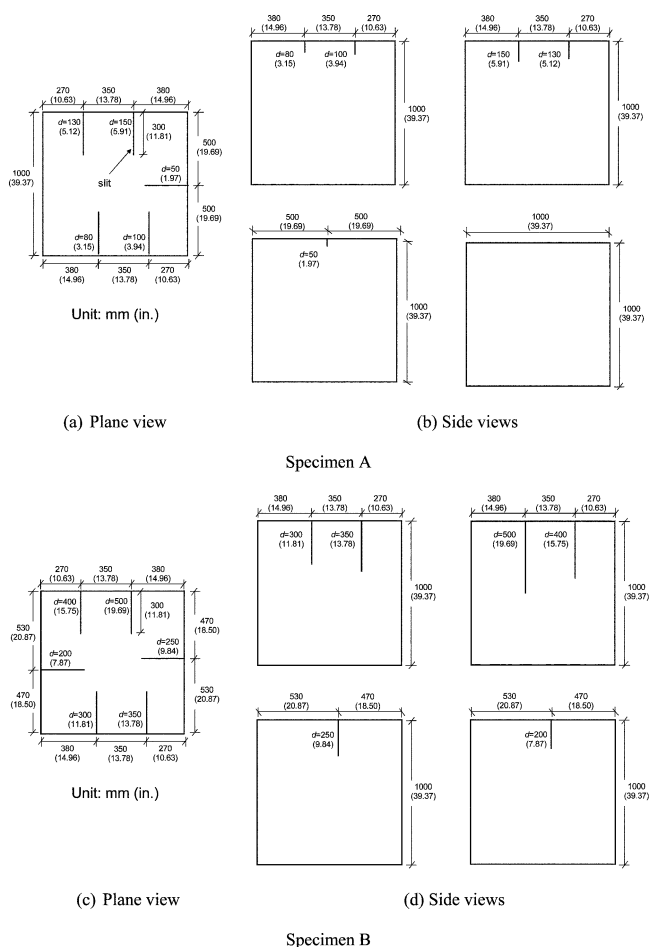


Fig. 1—Plane and side views of specimens indicating locations of slits and their depths.

in JIS A1108 and JSCE-G 502, using cylindrical specimens prepared in accordance with JIS A1132.

### Items of investigation

In the experiment, stress waves were generated by hammer impacts on one side of the slit and were received on the other side. To evaluate R-wave attenuation in association with scattering by a slit, the change of R-wave amplitude was examined and its correlation with the slit depth was established. For validating the feasibility of the correlation for slit depth estimation, similar testing procedures were conducted and the results compared with those acquired by the conventional P-wave TOF method.

### Testing

A two-sensor setup was configured for the testing. Figure 2 shows the schematic diagram for sensor arrangement as well as the actual test view. Two accelerometers with a flat response up to 30 kHz were attached to the top surface of the specimen, at 150 mm (5.91 in.) away from the specimen edge and 100 mm (1.97 in.) away from the slit, resulting in allocating a 200 mm (11.81 in.) spacing between the two sensors. Each sensor was fixed by a screw to a small steel plate of 10 x 30 x 30 mm (0.39 x 1.18 x 1.18 in.), which was later bonded to the concrete surface using high-vacuum wax as the coupling agent. A multi-channel data acquisition system was used to sample data at an interval of 5  $\mu$ s for a period of 0.02 seconds.

Throughout the experiment, hammer impacts were conducted by the same operator to minimize inconsistencies in the generation of stress waves. Generations of elastic waves were carried out by mechanical impacts with steel-ball hammers of different ball diameters: 5, 8, 11, 15, 25, and 35 mm (0.20, 0.31, 0.43, 0.59, 0.98, and 1.38 in.) (refer to Fig. 3). The purpose of using hammers of different ball diameters was to generate R-waves of different peak frequencies for investigations on the relations between wavelength, slit depth, and change in amplitude. Impacts were made at a distance of 100 mm (1.97 in.) from the sensor acting as the source to record waveform before the slit, as shown in Fig. 2. The sensor mounted on the other side of the slit would act as the receiver to record the changed waveform. For each hammer size, a total of five impacts were made on one side of the slit continuously, with an interval between two impacts of approximately 0.5 seconds. A total time length of approximately 3 seconds was required to record all the five waveforms before the acquisition was terminated and resumed for recording a new set of waveforms by impacts at the next location. The waveforms were stacked to enhance signal consistency as well as the sound-to-noise ratio. With the source-receiver sensors inverted, impacts and stacking of waveforms were then conducted for the other side of the slit. This resulted in two sets of stacked data for each hammer size for each slit. A similar sensor setup and measurement procedures were performed on the sound portion of Specimen A.

## EXPERIMENTAL RESULTS AND DISCUSSION

### Waveforms

Before applying further signal processing, all waveforms acquired were prefiltered by a tenth-order low-pass filter in accordance to the theoretical response of the sensor. Figure 4 shows a typical waveform that has been filtered. The waveform can be characterized by the initial arrival of

the P-wave, followed by strong bursts in the negative and positive phases indicating the arrival of the R-wave.<sup>20,21</sup> High amplitudes of the R-wave provide evidence that it carried a majority of the wave energy.<sup>9</sup> In the experiment, the velocities for P-waves and R-waves were determined by measuring the time lag between source and receivers mounted on the sound portion. Figure 5 gives examples of typical waveforms recorded by the source and receivers for different slit depths, which were generated by the hammer with a ball diameter of 8 mm (0.31 in.). For the sound

**Table 1—Concrete mixture proportions**

Cement, kg/m <sup>3</sup> (lb/ft <sup>3</sup> )	Water, kg/m <sup>3</sup> (lb/ft <sup>3</sup> )	w/c, %	Entrained air, %	Crushed stone, kg/m <sup>3</sup> (lb/ft <sup>3</sup> )	Siliceous sand, kg/m <sup>3</sup> (lb/ft <sup>3</sup> )	Air-entrained admixture, kg/m <sup>3</sup> (lb/ft <sup>3</sup> )
338 (21.10)	53.5 (3.34)	46.8	4.5	959 (59.87)	819 (51.13)	3.38 (0.21)

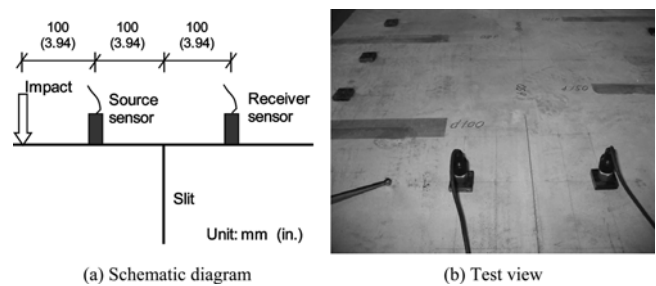


Fig. 2—Sensor arrangement and impact location.

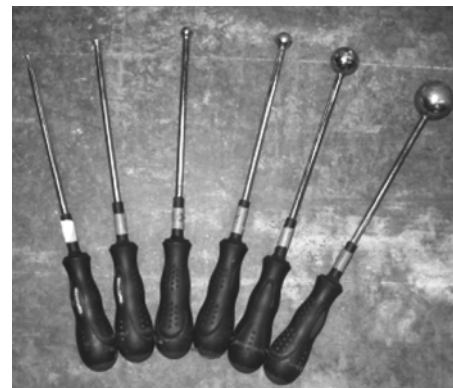


Fig. 3—Steel ball hammers used for generation of stress waves.

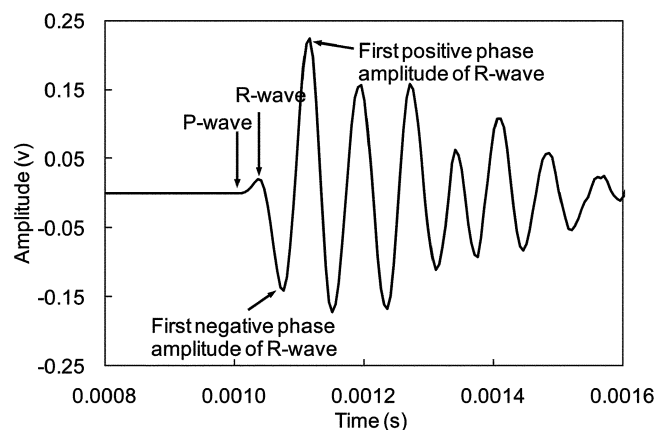


Fig. 4—Typical waveforms recorded from receiver.

portion, it was noticed that the waveform of the receiver had a lower amplitude compared to that of the source. The amplitude decay was caused by attenuation attributed to geometric spreading of the wavefront. For measurement surfaces with slits, greater amplitude decay can be observed in the waveforms. This is because when the waves impinged on the free surface of a slit, a portion of the waves was reflected back, and another portion passed through below the slit. The waves that impinged on the tip of the slit were then diffracted or scattered.<sup>22</sup> Therefore, the waves received by the sensor on the other side of slit have much lower energy, characterized by a decrease in amplitudes. Specifically, it can be seen from Fig. 5 that wave amplitude decreases with slit depth, inferring that the loss of wave energy becomes greater as the slit depth increases.

### Estimations by P-wave TOF

The P-wave TOF method estimates the depth of a surface-opening crack by considering the time required for P-waves to propagate from an impact source to a receiving point. The waves detected on the forward side of a crack are usually considered as those having been diffracted from the crack

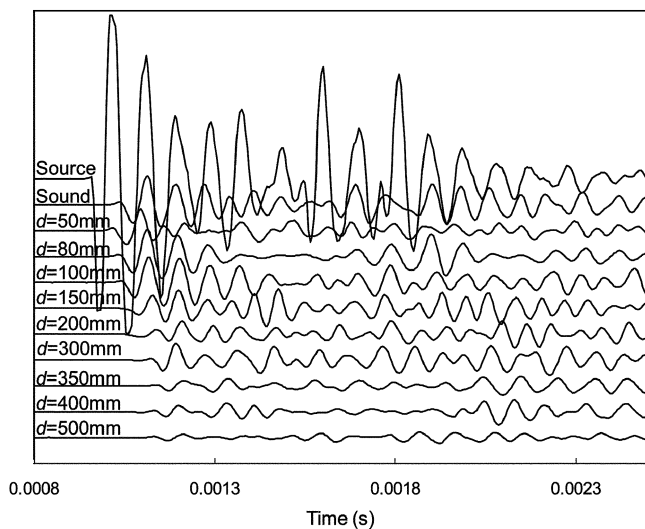


Fig. 5—Examples of waveforms recorded from impacts by 8 mm (0.314 in.) ball hammer. (Note: 1 mm = 0.0394 in.)

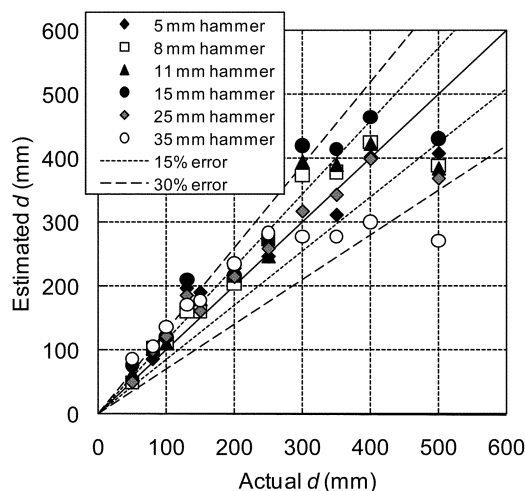


Fig. 6—Results of depth estimation by P-wave time-of-flight method. (Note: 1 mm = 0.0394 in.)

tip. In this current study, by considering the trigonometry relations between impact point, sensor distance and slit depth, the depth of a slit was obtained by solving the following

$$\sqrt{d^2 + 0.04} + \sqrt{d^2 + 0.01} - C_p \cdot \Delta t - 0.1 = 0 \quad (1)$$

where  $C_p$  is the P-wave velocity of sound concrete (m/second) (1 m/second = 3.281 ft/second); and  $\Delta t$  is the time difference of detected waves from the source and receiver, in seconds.

Estimation results by all the hammers are plotted in Fig. 6. From Fig. 6, it can be noted that the discrepancies between the estimated and actual values for shallower slits are relatively small. For greater depths, however, underestimation seemed to occur. Particularly, most of the estimation results for slits with depths  $\geq 300$  mm (11.81 in.) did not indicate a significant difference between each other. This trend could probably be explained by considering the three-dimensional half space in which elastic waves propagate. For a slit with depth considerably greater than the distance from sensor to slit end on the measured surface, the first arriving wave could be that having traveled and diffracted by the slit end on the measured surface. It was also possible that the first arriving wave has traveled in other shorter paths at subsurface concrete, rather than from below the slit. This means that the deeper the slit, the higher the possibility for erroneous detection because the energy of the desired first arrival becomes insignificant compared to those coming from other travel paths. The finding from this current study thus revealed potential problems that might occur when assessing cracks with limited dimensions using the P-wave TOF method, particularly those with a very short distance between the sensor and crack end on the measurement side. Under this circumstance, careful considerations are essential to anticipate propagation behavior of elastic waves with regard to the dimensions of crack and to identify potential boundary conditions that could affect the reliability of the assessment.

### Amplitude decay of R-wave

By using the recorded waveforms in time domain, amplitude factor  $F$ , defined as the ratio between R-wave amplitude of the receiver and the source, was calculated for each slit under different sizes of hammer. The amplitudes of interest were those detected immediately next to the first P-wave arrival (refer to Fig. 4), in both the positive and negative phases. These amplitudes were chosen for consideration because they were yet to be “contaminated” due to convergence of energy by other wave components as a consequence of complex interactions at the specimen boundary. The amplitudes of the first arriving R-wave was characterized by pronouncedly high magnitudes compared to the amplitude of first arriving bulk waves. Thus, the identifications for these R-wave amplitudes were relatively easy and errors in reading could be minimized.

To eliminate the effect of attenuation due to the geometric spreading of waves, values of  $F$  obtained from slit measurements were divided with that taken from the sound portion to derive the normalized amplitude factor  $F_{nor}$  for each slit depth and hammer size. Besides, to minimize discrepancy due to sensor fixing and coupling condition,  $F_{nor}$  obtained from both sides of the slit was then averaged by multiplying the obtained values with each other and then taking the square root of the multiplied product.

To define a normalized parameter that can address all crack depths, it was desirable that  $d$  be divided with the wavelength of R-wave,  $\lambda$ . In the case for impact-generated elastic waves,  $\lambda$  is usually referred to as the dominant wavelength, which can be calculated by using the common relation between velocity, wavelength, and central frequency  $f_c$ , which represents the frequency of waves that possesses the most energy and is most likely to influence the behavior of a medium. Parameter  $f_c$  can also be understood as the center of the area of the power spectrum density magnitude plot acquired from the fast Fourier transform (FFT). The FFT was performed with 512 samples and by applying the Hanning window to minimize spectral leakage. Values of  $f_c$  for each hammer size were calculated using the following equation

$$f_c = \frac{\sum_{k=0}^{N/2} \frac{1}{2} \cdot |X(f_k)|^2 \cdot f_k}{\sum_{k=0}^{N/2} \frac{1}{2} \cdot |X(f_k)|^2} \quad (2)$$

where  $X(f_k)$  is the FFT of the waveform at frequency  $f_k$ , and  $N$  is the number of discrete time samples. A typical power spectrum density plot of stress waves generated by the 15 mm (0.59 in.) steel-ball hammer is shown in Fig. 7. The measured R-wave velocities and calculated  $f_c$  for different sizes of steel-ball hammers are summarized in Table 2. These values were used to compute the ratio between slit depth and dominant wavelength  $d/\lambda$  for respective cases of hammer impact.

In this study, the relations between  $F_{nor}$  and  $d/\lambda$  were investigated by taking into account three separate cases of amplitudes: 1) positive phase amplitude; 2) negative phase amplitude; and 3) average of the absolute values of the positive and negative phase amplitudes. It was found from the waveform that the identification for the positive amplitude was the least ambiguous and its consistency could ensure the reliability of the correlation. An exponential regression was derived with the data of the positive phase amplitude, as plotted in Fig. 8. A reasonably good correlation ( $R^2 = 0.81$ ) was obtained, which can be expressed as

$$d = -0.481 \cdot \ln \frac{F_{nor}}{0.930} \cdot \lambda \quad (3)$$

From the correlation, it is found that as  $d/\lambda$  increases from 0 to 1, the decrease in  $F_{nor}$  is large, which is from 0.93 to 0.12, whereas for  $F_{nor}$  greater than 1, the variation in  $F_{nor}$  becomes much less significant. To explain this, common understandings about R-wave propagation behavior were adopted. It is known that the effective penetration depth of R-waves is approximately one wavelength. In other words, R-waves with wavelengths greater than the slit depth can be assumed to be propagating in a straightforward path below the slit. On the contrary, for R-waves with wavelengths shorter than the slit depth, propagation in less direct paths might take place, for example, along the slit surface and downward before being scattered at the slit end. To avoid errors in data interpretation, it is essential to examine the dominant wavelength of the excited R-waves and

adopt careful considerations for the possibility of a different propagation manner.

## REPEATABILITY AND VALIDITY OF METHODOLOGY

Using the same specimens, similar test procedures were repeated to validate Eq. (3) for estimating slit depth. Stress waves were generated by using the 8, 25, and 35 mm (0.31, 0.98, and 1.38 in.) steel-ball hammers. By adopting the same signal processing and data analysis procedures as stated in the previous section,  $F_{nor}$  values for the positive amplitude were obtained. The estimation results were plotted against the actual slit depths for comparison, as shown in Fig. 9. The

**Table 2—Velocity and  $f_c$  of R-waves generated by steel-ball hammers of different sizes**

Hammer diameter, mm (in.)	Velocity, m/second (ft/second)	Central frequencies $f_c$ , kHz
5 (0.20)	2374 (7789)	19.10
8 (0.31)	2176 (7139)	11.19
11 (0.43)	2280 (7480)	10.90
15 (0.59)	2210 (7250)	9.32
25 (0.98)	2247 (7372)	6.49
35 (1.38)	2407 (7897)	4.48

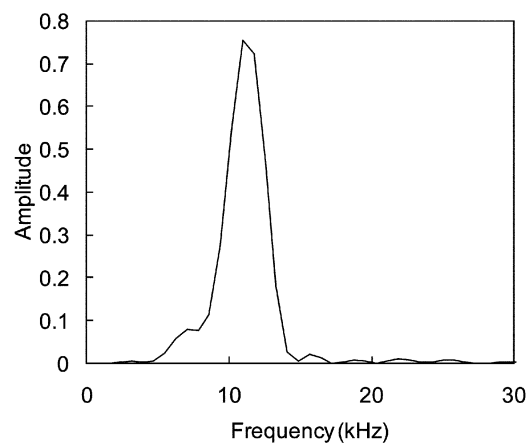


Fig. 7—Typical power spectrum density plot of stress waves generated by 15 mm (0.59 in.) steel ball hammer.

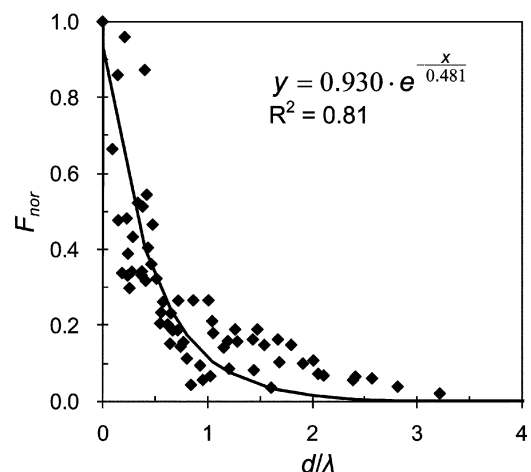


Fig. 8— $F_{nor}$  versus  $d/\lambda$  for positive phase R-wave amplitude.

estimations by the 25 and 35 mm (0.98 and 1.38 in.) steel-ball hammers gave satisfactory accuracy in general. Most of the results were found to be within the  $\pm 15\%$  error range. On the other hand, in examining the estimations by the 8 mm (0.31 in.) steel-ball hammer, apparent discrepancies were found, especially for plots with regard to  $d$  of 200 mm (11.81 in.) and

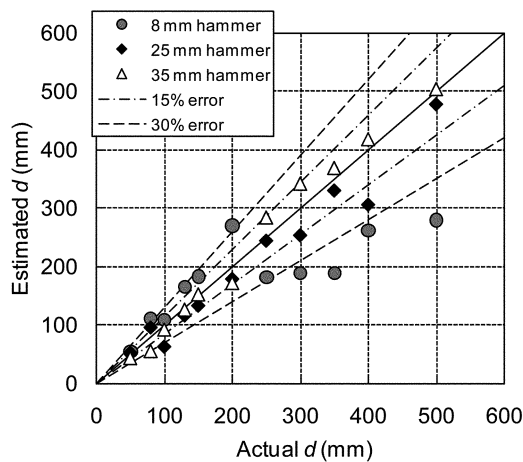


Fig. 9—Estimation results by proposed R-wave methodology. (Note: 1 mm = 0.0394 in.)

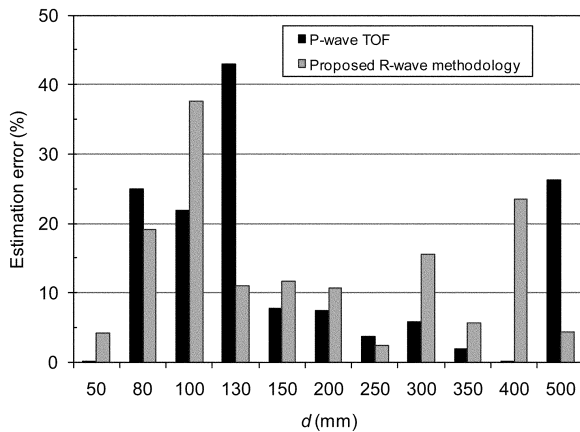


Fig. 10—Comparison between estimation error by P-wave time-of-flight and proposed R-wave methodology (25 mm [0.98 in.] steel-ball hammer). (Note: 1 mm = 0.0394 in.)

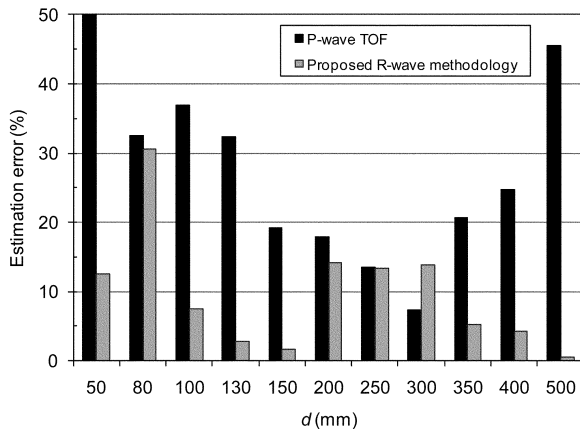


Fig. 11—Comparison between estimation error by P-wave time-of-flight and proposed R-wave methodology (35 mm [1.38 in.] steel-ball hammer). (Note: 1 mm = 0.0394 in.)

greater. The 8 mm (0.31 in.) steel-ball hammer tended to generate R-waves of relatively higher  $f_c$ , with  $\lambda$  shorter than the  $d$  of some of the slits in the specimens. Therefore, the results justified that for deeper slits, which yield  $d/\lambda$  values greater than 1, estimations for  $d$  become unreliable because the R-waves have propagated in a different manner.

Figures 10 and 11 compare the estimation errors between the P-wave TOF and the proposed R-wave methodology for the 25 and 35 mm (0.98 and 1.38 in.) steel-ball hammers, respectively. Generally, there is no consistent trend in firmly inferring the superiority of the proposed methodology compared to the P-wave TOF method. With the proposed methodology, however, the 35 mm (1.38 in.) steel-ball hammer seemed to be able to give more accurate estimations for almost all slit depths. This suggested that large wave energy and long wavelength should be preferred for better results. On the other hand, acquisition of data by different sizes of steel-ball hammers is also essential for comparison purposes to enhance the accuracy of estimation. With the findings of this study, the feasibility of the proposed methodology in estimating depths of concrete cracks with reasonable accuracies can be confirmed.

## CONCLUSIONS

R-waves generated by impacts using steel-ball hammers were used to characterize surface-opening cracks in concrete. Cracks in the form of vertical slits with depths ranging from 50 to 500 mm (1.97 to 19.69 in.) were introduced in the specimens. Based on the results of the experimental investigation, the following conclusions are drawn:

1. Due to reflection, diffraction, and scattering, attenuation of stress waves became greater with the increase in slit depth. The tendency in which the first arriving R-wave amplitudes decrease with an increase in the slit depth was also noticed.

2. The accuracy of estimation by the P-wave TOF method decreased with slit depth. For slits with depths significantly greater than the distance between sensor and slit end on the measured surface, it was highly possible that P-waves propagating the measured surface or subsurface concrete could be mistaken as the first arrival that have traveled from below the slit. The deficiency of the P-wave TOF method was thus demonstrated. Based on the findings, the method becomes less reliable when the crack depth is equivalent to or exceeds the distance between sensor and crack end on the attachment surface.

3. Taking into consideration the decay of R-wave amplitude in the positive phase, a reasonable exponential correlation between the amplitude factor and slit depth-to-dominant wavelength ratio was established. From the correlation, it can be noted that for  $d/\lambda$  greater than approximately 1, the decrease of  $F_{nor}$  with an increase of  $d/\lambda$  is less noticeable compared to that for  $d/\lambda$  less than 1. This implies that if the magnitude of dominant wavelength is greater than the slit depth, a more accurate estimation can be expected.

4. The results of repeated measurements by the 25 and 35 mm (0.98 and 1.38 in.) steel-ball hammers validated the proposed methodology and the relevant constants of expressions used for calculating slit depth. The results also indicated that with the proposed method, accuracy of estimations improved with the size of the steel-ball hammers.

## FURTHER RESEARCH

The current study adopted a two-sensor approach for characterizing surface-opening cracks in concrete. To

develop a simple and effective methodology to be applied in-place, it is desirable to develop procedures that predict the curvature or inclination of cracks that are not completely vertical in nature. This can be realized by a multi-sensor array approach to first predict the orientation of cracks, followed by exploiting the decay of R-wave amplitudes in a quantitative way for estimating crack depth. Further experiments on different types of specimens are required for data accumulation and establishment of amplitude-crack depth relations to account for various geometrical boundary conditions. In addition, a more steady method should be developed to excite R-waves, for example, in the form of a mechanical instrument that instigates tapings with a constant force at a consistent location. Field measurements should also be carried out to further justify the reliability of the proposed methodology through verifications by other methods such as concrete coring.

### ACKNOWLEDGMENTS

This work was supported under Grant-in-Aid for Young Scientific Research (Start-up) No. 20860100 by the Japan Society for the Promotion of Science. We are also grateful to K. Tazaki of Nagaoka University of Technology for his effort during specimen preparation and testing.

### REFERENCES

1. Neville, A. M., *Properties of Concrete*, fourth edition, Addison Wesley Longman Ltd., Essex, UK, 1997, 844 pp.
2. Van Hauwaert, A.; Thimus, J. F.; and Delannay, F., "Use of Ultrasonics to Follow Crack Growth," *Ultrasonics*, V. 36, 1998, pp. 209-217.
3. Sakata, Y., and Ohtsu, M., "Crack Evaluation in Concrete Members Based on Ultrasonic Spectroscopy," *ACI Materials Journal*, V. 92, No. 6, Nov.-Dec. 1995, pp. 686-698.
4. Chang, Y. F., and Wang, C. Y., "A 3-D Image Detection Method of a Surface Opening Crack in Concrete Using Ultrasonic Transducer Arrays," *Journal of Nondestructive Evaluation*, V. 16, No. 4, 1997, pp. 193-203.
5. Lin, Y., and Su, W. C., "The Use of Stress Waves for Determining the Depth of Surface-Opening Cracks in Concrete Structures," *ACI Materials Journal*, V. 93, No. 5, Sept.-Oct. 1996, pp. 494-505.
6. Liu, P. L.; Tsai, C. D.; and Wu, T. T., "Imaging of Surface-Breaking Concrete Cracks Using Transient Elastic Waves," *NDT&E International*, V. 29, No. 5, 1996, pp. 323-331.
7. Sansalone, M.; Lon, J. M.; and Streett, W. B., "Determining The Depth of Surface-Opening Cracks Using Impact Generated Stress-Waves

and Time-of-Flight Techniques," *ACI Materials Journal*, V. 95, No. 2, Mar.-Apr. 1997, pp. 168-177.

8. Naik, T. R., and Malhorta, V. M., "The Ultrasonic Pulse Velocity," CRC Handbook on Nondestructive Testing of Concrete, V. M. Malhorta and N. J. Carino, eds., CRC Press, FL, 1991, pp. 169-188.

9. Hevin, G.; Abraham, O.; Pedersen, H. A.; and Campillo, M., "Characterization of Surface Cracks with Rayleigh Waves: A Numerical Model," *NDT&E International*, V. 31, No. 4, 1998, pp. 289-297.

10. Zerwer, A.; Polak, M. A.; and Santamarina, J. C.; "Detection of Surface Breaking Cracks in Concrete Members Using Rayleigh Waves," *Journal of Environmental and Engineering Geophysics*, V. 10, No. 3, 2005, pp. 295-306.

11. Aggelis, D. G.; Shiotani, T.; and Polyzos, D., "Characterization of Surface Crack Depth and Repair Evaluation Using Rayleigh Waves," *Cement and Concrete Composites*, V. 31, No. 1, 2009, pp. 77-83.

12. Doyle, P. A., and Scala, C. M., "Crack Depth Measurement by Ultrasonics: A Review," *Ultrasonics*, V. 16, No. 4, 1978, pp. 164-170.

13. Shiotani, T., and Aggelis, D. G., "Evaluation of Repair Effect for Deteriorated Concrete Piers of Intake Dam Using AE Activity," *Journal of Acoustic Emission*, V. 25, 2008, pp. 69-79.

14. Tsutsumi, T.; Wu, J.; Huang, X.; and Wu, Z., "Introduction to A New Surface-Wave Based NDT Method for Crack Detection and Its Application in Large Dam Monitoring," *Proceedings of International Symposium on Dam Safety and Detection of Hidden Troubles of Dams and Dikes*, Xian, China, 2005. (CD-ROM).

15. Massery, B., and Mazza, E., "Analysis of The Near-Field Ultrasonics Scattering at A Surface Crack," *Acoustical Society of America Journal*, V. 118, No. 6, 2005, pp. 3585-3594.

16. Masserey, B., and Mazza, E., "Ultrasonic Sizing of Short Surface Cracks," *Ultrasonics*, V. 46, 2007, pp. 195-204.

17. Jian, X.; Dixon, S.; Guo, N.; Edwards, R. S.; and Potter, M., "Pulsed Rayleigh Wave Scattered at a Surface Crack," *Ultrasonics*, V. 44, 2006, pp. 1131-1134.

18. Okada, K.; Ito, K.; Fuwa, A.; and Hirasawa, I., *Reinforced Concrete Engineering*, Kajima Institute Publishing Co. Ltd., Tokyo, Japan, 2003, 274 pp. (in Japanese)

19. BS 8110-1, "Structural Use of Concrete: Code of Practice for Design and Construction," British Standards Institution, London, UK, 1997, 168 pp.

20. Sansalone, M. J., and Streett, W. B., "Impact-Echo Nondestructive Evaluation of Concrete and Masonry," Bullbrier Press, Ithaca, NY, 1997, 339 pp.

21. Luo, Q., and Bungey, J. H., "Using Compression Wave Ultrasonic Transducers to Measure the Velocity of Surface Waves and Hence Determine Dynamic Modulus of Elasticity for Concrete," *Construction and Building Materials*, V. 10, No. 4, 1996, pp. 237-242.

22. Yew, C. H.; Chen, K. G.; and Wang, D. L., "An Experimental Study of The Interaction between Surface Waves and a Surface Breaking Crack," *Journal of Acoustic Society of America*, V. 75, No. 1, 1984, pp. 189-196.